OPTIC BREAKDOWN IN RUBY AND RELATED EFFECTS

T. P. BELIKOVA, A. N. SAVCHENKO, and É. A. SVIRIDENKOV

P. N. Lebedev Physics Institute, Academy of Sciences, USSR

Submitted July 14, 1967

Zh. Eksp. Teor. Fiz. 54, 37–45 (January, 1968)

Luminescence, multiphoton absorption, photoconductivity, and breakdown accompanied by shock wave are observed when ruby is irradiated by a high-power ruby laser pulse. A mechanism of light-induced breakdown in transparent solids is proposed demonstrating the important role of electron transitions in the absorption of light by free charge carriers. The coefficient of multiphoton absorption, temperature, and pressure in the shock wave are evaluated.

INTRODUCTION

IT is shown in[1] that the beam of a high-power ruby laser focused inside a ruby specimen causes luminescence when the power is $W \sim 10^8-10^9$ w/cm^2, and breakdown when the power is increased above 10^{10} w/cm^2. It is further suggested that the luminescence and breakdown are caused by multiphoton excitation and ionization of the chromium in the ruby. The free carriers that appear in the conductivity band absorb laser radiation, heat up, ionize the corundum lattice, and cause an avalanche breakdown, a process similar to that occurring in gases[2].

Experiments aimed at detecting multiphoton absorption and photoconductivity of ruby[3] were carried out to verify this hypothesis. The present paper describes these experiments in greater detail than do the preliminary reports[1,3] and gives new results from the observation of shock waves accompanying ruby breakdown.

1. MULTIPHOTON ABSORPTION AND LUMINESCENCE

The ruby specimens (20 × 6 × 6 mm) containing 0.05% chromium were placed in the focus of the beam from a high-power Q-switched ruby laser. With an irradiation power $W \sim 10^8$ w/cm^2 we observed a luminescence band with a maximum at $\lambda \approx 625$ nm (Fig. 1, curve 1); when the power was increased by an order of magnitude, an additional blue luminescence band with a maximum at $\lambda \approx 450$ nm was observed (Fig. 1, curve 2).

The luminescence spectra were recorded by a quartz spectrograph with a power 1 : 3; the scattered generation light was eliminated by a filter containing copper sulfate solution. The light of the pump lamp was passed through a KS-19 filter that was well matched to the copper sulfate filter. The spectrum was calibrated against the density of photographic film. The standard light source was a ribbon lamp with a known color temperature. The energy emitted by the luminescence bands was determined from the density of the film and reached $E_l \sim 10^{-5}-10^{-6}$ J for an incident energy E ~ 1 J. The incident energy was determined with a calorimeter and the power by measuring the generation pulse length with an S1-11 oscilloscope. The beam cross section in the focal region was determined from the beam divergence. The space-time structure of the beam was not considered. This may have changed our results by a factor of several units.

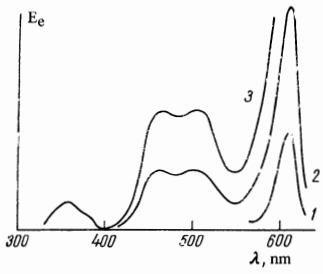

FIG. 1. Ruby luminescence spectrum at various irradiation powers (plots are numbered according to increasing power).

An irradiation power $W > 10^{10}$ W/cm^2 caused a breakdown within the specimen at the focus of the lens and damaged the ruby[1]. The breakdown was accompanied by a strong light flash. The spectrum of the flash is given in Fig. 1 (curve 3); it contains an ultraviolet band with a maximum at $\lambda \approx 360$ nm in addition to the luminescence bands described above.

We assume that these effects are due to multiphoton absorption. Multiphoton absorption in chromium and free carrier absorption are manifested by the dependence of the absorption coefficient of the ruby on the intensity of the incident light. The following experiment was performed to measure this dependence and to detect directly the carriers in the conductivity band of corundum (see Fig. 2).

The light of Q-switched ruby laser 1 was focused in ruby specimen 4. Saturable filter 2 (a cryptocyanine solution in our case) was used as the Q-switch. The absorption coefficient in ruby was measured with differential difference amplifier 7. The amplifier separated out the difference between the signals from the photomultipliers FÉU-I and FÉU-II that detected the light transmitted by the ruby and the laser light split off by semitransparent mirror 3 respectively. The amplified difference signal was fed to one beam of an S1-7 two-beam oscilloscope (OI in Fig. 2), while the other beam was driven by the amplified signal from the photomultiplier FÉU-II. The light beams incident on the photomultipliers

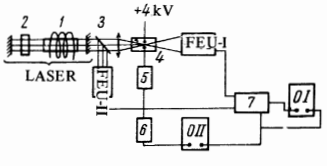

FIG. 2. Experimental setup for measuring ruby absorption coefficient and photoconductivity (designations are given in text).

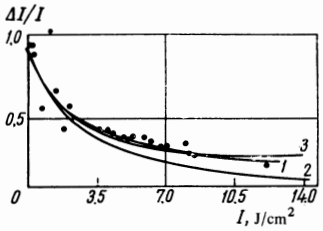

FIG. 3. Ruby absorption coefficient as a function of incident light intensity. Points and plot 1 represent experimental data, plots 2 and 3 represent theoretical data.

were adjusted with neutral filters to obtain a precise balance of both channels of amplifier 7.

The difference Δ I between signals from the photomultipliers FÉU-II and FÉU-I determined the light absorption in the ruby at the generation wavelength. The ratio of this difference to the intensity of incident light, I = Δ E/S, determined the absorption in the specimen. Figure 3 shows the resulting dependence of ΔI/I on the incident radiation intensity (curve 1). The decreasing absorption in ruby with increasing irradiation density is due to the bleaching of the ruby stemming from equalization of the populations at the ground and excited levels.

Let us see what form the absorption curve should take with allowance for the bleaching of the ruby. We denote the ground level population by n_1, the excited level population by n_2, and their difference by $n_2 - n_1 = N$. When light with intensity I = f(t) passes through the ruby, absorption from the ground level occurs with a probability $n_1\sigma I(t)$ (where σ is the absorption cross section for the working transition), and stimulated emission with a probability $n_2\sigma I(t)$. Spontaneous emission can be neglected during the pulse length $\tau \sim 10^{-8}$ sec, because the lifetime of the particles at the excited level is $\tau_0 = 3 \times 10^{-3}$ sec. In this case the balance equation for the number of particles has the form

$$dN / dt = -2N\sigma I(t) \tag{1}$$

and the attenuation of the light by the ruby is given by

$$\partial I / \partial x = N\sigma I.$$

Since the length of the ruby l = 2 cm is less than the reciprocal absorption coefficient, the quantity $\int(\partial I/\partial x)\partial x$ is from now on replaced by ΔI. The shape of the incident light pulse is assumed Gaussian:

$$I(t) = I_0 \exp\left(-\frac{1}{2}\left|\frac{t}{\tau}\right|^2\right). \tag{2}$$

The time constant of our apparatus was larger than the pulse length, so that we actually measured the quantity

$$\int_{-\infty}^{\infty} \Delta I dt.$$

The following dependence of the measured absorption is obtained from (1) and (2):

$$\int_{-\infty}^{\infty} \Delta I(t)\,dt \Big/ \int_{-\infty}^{\infty} I(t)\,dt = \frac{N\sigma}{\sqrt{2\pi}} \int_{-\infty}^{\infty} \left[\exp\left(-\frac{1}{2}\left|\frac{t}{\tau}\right|^2\right) + 2I_0\sigma \int_{-\infty}^{t} \exp\left(-\frac{1}{2}\left|\frac{t'}{\tau}\right|^2\right) dt' \right] dt. \tag{3}$$

This dependence is given in Fig. 3 (curve 2). We see that the curve lies substantially below the experimental plot. The discrepancy increases with increasing intensity of incident light. This means that we observed an additional absorption that was not taken into account by our equations for a two-level system and that increased with the intensity of light. We assume that this absorption is due to multiphoton transitions from the excited level.

The transmission of light through the ruby, taking two-photon absorption from the excited level into account, is defined by the following equations:

$$\frac{dn_1}{dt} = -n_1\sigma I + n_2\sigma I, \tag{4a}$$

$$\frac{dn_2}{dt} = n_1\sigma I - n_2\sigma I - n_2\gamma I^2 + n_3\gamma I^2 + n_3 w_3, \tag{4b}$$

$$\frac{dn_3}{dt} = n_2\gamma I^2 - n_3\gamma I^2 - n_3 w_3, \tag{4c}$$

$$\frac{1}{c}\frac{dI}{dt} + \frac{dI}{dx} = n_1\sigma I - n_2\sigma I - n_2\gamma I^2 + n_3\gamma I^2. \tag{4d}$$

here γ is the cross section of two-photon absorption from level 2 to level 3. The last two terms of (4b) determine the stimulated two-photon emission and the relaxation from level 3. These can be neglected since the energy involved in our experiment is not high enough to cause saturation of the two-photon transition. We compute n_3/n_2 from the experimental data and find that $n_3/n_2 < 0.05$. The absorption as a function of incident light intensity according to (4a) and (4b) has in this case the following form (for a Gaussian incident pulse)

$$\int_{-\infty}^{\infty} \Delta I dt \Big/ \int_{-\infty}^{\infty} I\,dt = \frac{N_0}{\sqrt{2\pi}} \int_{-\infty}^{\infty} \left\{ 1 - \int_{-\infty}^{t} I_0^2\sigma \exp\left[-\left|\frac{t'}{\tau}\right|^2 - 2\sigma I_0 \int_{-\infty}^{t'} \exp\left(-\frac{1}{2}\left|\frac{t''}{\tau}\right|^2\right) dt'' - \gamma I_0^2 \int_{-\infty}^{t'} \exp\left(-\left|\frac{t''}{\tau}\right|^2\right) dt'' \right] dt' \right\} \cdot \exp\left(-\frac{1}{2}\left|\frac{t}{\tau}\right|^2\right) \left\{ \sigma \exp\left[-2\sigma I_0 \int_{-\infty}^{t} \exp\left(-\frac{1}{2}\left|\frac{t'}{\tau}\right|^2\right) dt' - \gamma I_0^2 \int_{-\infty}^{t} \exp\left(-\left|\frac{t'}{\tau}\right|^2\right) dt' \right] + \gamma I_0 \exp\left(-\frac{1}{2}\left|\frac{t}{\tau}\right|^2\right) \left[1 - \exp\left(-2\sigma I_0 \int_{-\infty}^{t} \exp\left(-\frac{1}{2}\left|\frac{t'}{\tau}\right|^2\right) dt'\right) \right] \right\} dt. \tag{5}$$

The numerical values obtained from (5) by the M-20 computer were used to select points for a plot that would coincide with the experimental curve (Fig. 3, curve 3). The curve was then used to determine the numerical value of $\gamma/\sigma^2\tau$, which was found to be 0.2. The coefficient of two-photon absorption was equal to $k = 2 \times 10^{-3}$ cm^{-1} at an irradiation power $W \sim 10^8$ w/cm^2. Consequently for this power $\sim 10^{-3}$ of the incident energy is absorbed along l = 1 cm of ruby length. As noted above, $\sim 10^{-6}$ of the incident energy is transformed into luminescence and therefore the luminescence yield amounts to $\eta \sim 0.1\%$. This estimate may turn out to be too low because the possible contribution from free carrier absorption was not taken into account.

2. PHOTOCONDUCTIVITY OF THE RUBY AND BREAKDOWN

The photoconductivity of ruby observed by us verifies the presence of free carriers in the conductivity band. The experiment was performed in the following manner. Holes for electrodes 2 mm in diameter were drilled in the investigated ruby specimen (4 in Fig. 2). The distance between the capacitor plates formed by the electrodes was 2 mm. The laser light was focused into

the interelectrode space. A voltage of V = 4 kV was applied to the electrodes. The signal appeared across a resistor (R = 10 K) and was fed through amplifiers 5 and 6 (Fig. 2) to one beam of the S1-7 oscilloscope (OII in Fig. 2). A laser generation signal from the FÉU-II photomultiplier was supplied to the second beam of the oscilloscope.

Without protective measures the signal is several orders of magnitude larger than expected. This is due to surface conductivity. The effect is eliminated by a grounded metal ring fastened to the ruby around the electrode that supplies the signal. It is possible that the photoconductivity signal observed by Dneprovskiĭ and others[4], which exceeded the theoretical value by three orders of magnitude, was also due to surface conductivity. This is all the more probable because the field density was the same on the surface and within the specimen in[4], because it was illuminated by a parallel beam of light. In our experiment the field density was higher by an order of magnitude in the interelectrode space than on the surface.

A volume conductivity signal was observed when the irradiation power was $W \sim 10^{10}$ W/cm^2. Conductivity was observed in a very small interval of intensity variation of the incident light before the onset of damage[3]. We consider that this damage was caused by free-carrier absorption of light followed by the development of the breakdown.

As we know[5], the coefficient of free-carrier absorption is $K = 4\pi\mu/c$, where μ is the high-frequency conductivity due to these carriers. This quantity is determined by the following expression[5]:

$$\mu = \frac{Ne^2}{m\omega^2}\nu_{\text{eff}},$$

where N is the free-carrier concentration, ν_{eff} is the effective collision frequency, and ω is the frequency of light. According to our computation $\nu_{\text{eff}} \sim 10^{14}$ sec^{-1} for ruby. $K \sim 10^{-3}$ for a concentration $N \sim 10^{15}$ cm^{-3} corresponding to the pre-breakdown condition[3]; this means that the free-carrier absorption coefficient is comparable to the multiphoton absorption coefficient computed above.

The power lost by the light due to free-carrier absorption in ruby is

$$dW/dt = \mu\mathscr{E}^2,$$

where E is the light field intensity. The power acquired by a single electron amounts to

$$\frac{dE_e}{dt} = \frac{e^2\mathscr{E}^2}{m\omega^2}\nu_{\text{eff}}.$$

For the intensities used, $E = 3 \times 10^4$ cgs esu and we obtain $dE_e/dt \sim 1$ erg/sec, i.e. one electron in a time $t = 10^{-11}$ sec acquires an energy $E_e = 10^{-11}$ erg ~ 10 eV. This energy is a priori sufficient to ionize the corundum lattice whose forbidden gap width is $E_g \sim 8$ eV. It can be shown that with $E = 3 \times 10^4$ cgs esu the electron energy losses in lattice heating occur at a rate that is lower by an order of magnitude. Lattice ionization yields two new electrons and thus produces an avalanche process causing the breakdown in the material. This avalanche causes an almost total lattice ionization and total absorption of the remaining radiation during the lifetime of an electron in the band; as computed from effective mobility data[6], the electron lifetime is $\sim 10^{-9}$ sec. The energy absorbed in the breakdown is $E_{\text{abs}} \sim 0.1$ J for an incident energy of $E \sim 0.3$—0.5 J.

3. OBSERVATION OF SHOCK WAVES IN RUBY DAMAGE BY LIGHT

The absorption of large energy in a small ($V \sim 10^{-6}$ cm^{-3}) volume of the focal region of the lens results in a sharp rise of temperature and pressure in this volume. The rise in pressure creates a shock wave that propagates in the ruby. These shock waves were observed by us in the course of the following experiment (see Fig. 4).

The light of a Q-switched laser (4, 5, 6, 7) was focused by lens 10 within the ruby specimen 11. Lenses 10 and 10′ formed a telescopic system used to obtain a weakly divergent beam. The beam was directed into a delay line formed by mirrors 12 and 13. Movement of mirror 13 allowed us to vary the delay time from a few nanoseconds to 150 nsec. The light that passed through the delay line crossed ruby specimen 11 through the side walls, was focused by lens 14 onto diaphgram 15, and fell on photographic film 16. The film and the ruby specimen were in the conjugate planes of lens 14 at double the focal length. Diaphragm 15 cut off the generation light scattered by the ruby specimen and increased the image contrast of thoes eregions that had an altered refraction coefficient. Such regions deflected the transmitted light away from the aperture of diaphragm 15. The dimensions of the diaphragm were determined by the divergence of the laser beam and the focal length of lens 14. The system was aligned by a helium-neon laser 1 whose divergence was adjusted to match that of the ruby laser, using telescopic system 2, 2′ and diaphragm 3.

The system was further refined to observe a single breakdown at various time instants (Fig. 4b). A semitransparent mirror (12′) was placed across the light path in the delay line, creating its own beam with a shorter delay time. The second beam was focused by lens 14 onto its own aperture in the diaphragm; prism 17 placed in the path of this beam separated the images in the plane of film 16.

Figure 5 shows the photographs of various damage modes obtained at various time instants. Figure 6 shows photographs of damage regions obtained with two time

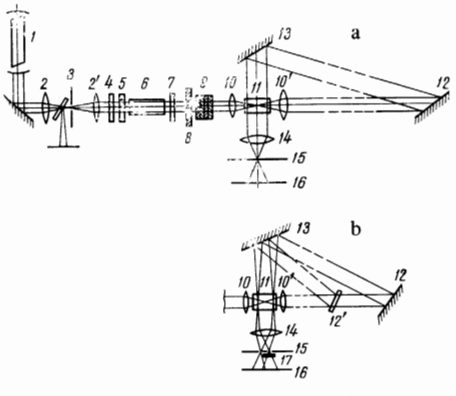

FIG. 4. Experimental setup for the study of shock waves in ruby under light-induced breakdown.

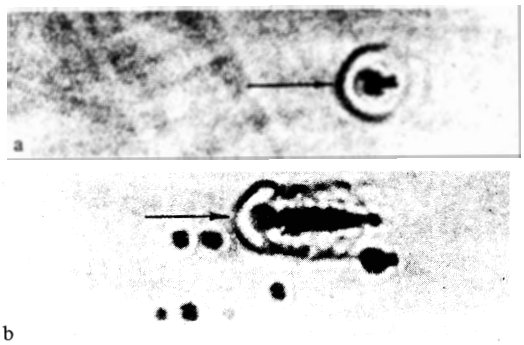

FIG. 5. Damage and shock waves in ruby with a time delay of 86 nsec.

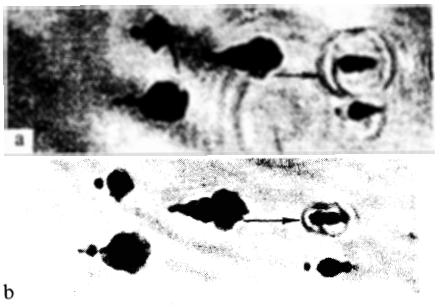

FIG. 6. Damage and shock waves in ruby with two time delays: a—40 nsec delay; b—86 nsec delay.

delays. In addition to the damage shadowgraphs, these photographs also show shock waves propagating from the damage point. Since each ruby specimen was used several times, the photographs show shadowgraphs of the previous damage events. The damage corresponding to the given time instant of the exposure is indicated by an arrow that also shows the direction of the incident light. If the power and energy of the incident pulse are significantly above the breakdown threshold, the damage propagates within the specimen, moving towards the beam. The velocity of propagation of the damage can be equal to that of the shock wave (Fig. 5a) or it can significantly exceed the latter. Figure 5b shows a cone formed by the envelope of shock wave fronts.

The measured velocities of shock waves depending on the energy absorbed in the damage volume lie within the limits of ~12—15 km/sec. These velocities correspond to the pressures at the shock wave front of P = (1.5—3) $\times 10^6$ kg/cm^2 and to temperatures T = (3—6) $\times 10^3$ °K determined from the shock adiabat of ruby[7]. The total energy in the shock wave is

$$U = \left[-\frac{1}{2} P \left(\frac{1}{\rho_0} - \frac{1}{\rho} \right) + 3N_a kT \right] V,$$

where ρ_0 and ρ are densities of unperturbed material and material in the shock wave, respectively, N_a is the atomic concentration, and V is the initial volume of the shock wave. The thermal portion of the energy $3N_akT$ is much smaller than the mechanical energy and can be neglected. The mechanical energy in the shock wave determined from this equation was $U_{mech} \sim 10^{-1}$ J in our experiments. This quantity coincides with energies we measured from absorption.

After the shock wave front passed, the particles of the material have a certain velocity directed along the radius away from the center. A decrease of temperature and expansion of the material create a negative pressure in the focal region leading to the formation of a cavity. This cavity can occur with or without cracking. The rate of transverse cracking depends on the energy absorbed in the breakdown region and varies from 2.7 km/sec in the initial phase to 0.27 km/sec 100 nsec later; it is thus much slower than the speed of sound in ruby. The motion of the damage region towards the beam can be due to the following causes. The shock wave favors the breakdown occurring in the wave front region that is irradiated with the laser beam; in this case the shock wave has a "detonating" nature. This mechanism explains the velocity of the damage region, which equals that of the shock wave (Fig. 5a), and does not explain a velocity that is ten times higher than that of the shock wave (Fig. 5b). Such a motion of the damage region can be due to the time-dependent rise of the generation pulse.

The intensity of radiation at a given instant of time varies in space within the crystal, and has a maximum in the focus. This is the site of the initial breakdown. As the generation pulse rises in time, the radiation intensity also increases in the region before the focus, exceeding the threshold at some point and causing a breakdown. The threshold intensity is then reached at a point further removed from the focus, etc. Such a process of intensity increase is limited by the time approximately equal to one-half the effective time of the generation pulse when the radiation intensity is increasing. If the energy density is not much lower on the surface than within the specimen, the breakdown also occurs on the surface, since the threshold for the surface breakdown is lower. This is apparently due to the photoeffect at the shallow traps in the surface layer of the crystal, leading to the formation of an electron cloud near the dielectric surface. It is apparently these electrons that are responsible for the large surface photoconductivity observed by us in the laser light. If the incident beam energy exceeds some critical value, the electron cloud becomes a plasma flare that absorbs the incident radiation. A shock wave arises within the flare and moves against the laser beam[8].

If the breakdown occurs on the back surface of the specimen, the shock wave enters the ruby as shown in Fig. 6. The predominant damage on the back surface while the breakdown occurs on both surfaces is due to the effect of this wave.

Bell and Landt[9] recently reported breakdown caused by a ruby laser beam on the surface of a platinum plate immersed in water. Shock waves with 500,000 atm pressure were observed in the water. Shock wave pressures of several million atm obtained in light-induced breakdown in solids may possibly be used to create and study phase transformations.

CONCLUSION

The above experiments demonstrate the important role of electron transitions and absorption of light by electrons in the processes of light-induced breakdown in corundum. Acoustic phonons generated in the course

of stimulated Mandel'shtam-Brillouin scattering cannot cause the destruction of corundum as suggested by Pashkov and Zverev[10], because the threshold of the stimulated Mandel'shtam-Brillouin scattering is much higher than that of the electron avalanche and also the stress in the acoustic wave is lower than the strength of corundum.

The breakdown mechanism proposed by us points to methods of increasing the power limit of ruby lasers and amplifiers. First, this calls for a reduction of the effective collision frequency by decreasing the temperature. According to computations, a temperature decrease to the nitrogen level doubles the power. Second, this requires a reduction in the pulse length beyond the limits of band lifetime of the electron, which in turn reduces the number of generations in the avalanche and prevents the development of the breakdown.

The authors thank M. D. Galanin for his attention and interest in this work and A. F. Suchkov for valuable discussions and help.

[1] T. P. Belikova and E. A. Sviridenkov, ZhETF Pis. Red. 1, 6, 37 (1965) [JETP Lett. 1, 6, 171 (1965)].

[2] Ya. B. Zel'dovich and Yu. P. Rayzer, Zh. Eksp. Teor. Fiz. 47, 1150 (1964) [Sov. Phys.-JETP 20, 772 (1965)].

[3] T. P. Belikova and E. A. Sviridenkov, ZhETF Pis. Red. 3, 394 (1966) [JETP Lett. 3, 257 (1966)].

[4] V. S. Dneprovskiĭ, D. N. Klyshko, and A. N. Penin, ZhETF Pis. Red. 3, 385 (1966) [JETP Lett. 3, 251 (1966)].

[5] T. S. Moss, Optical Properties of Semiconductors, London, 1959.

[6] Urs Erwin Hochuli, Phys. Rev. 133, A468 (1964).

[7] Handbook of Physical Constants, Ed. S. Clark, N. Y. 1966.

[8] S. A. Ramsden and W. E. Davies, Phys. Rev. Lett. 13, 227 (1964).

[9] C. E. Bell and J. A. Landt, Appl. Phys. Lett. 10, 46 (1967).

[10] V. A. Pashkov and G. M. Zverev, Zh. Eksp. Teor. Fiz. 51, 777 (1966) [Sov. Phys.-JETP 24, 516 (1967)].

Translated by S. Kassel
6